Pergamon

Int. J. Solids Structures Vol. 35, No. 14, pp. 1515–1532, 1998

0020-7683/98 $19.00 + .00

PII: S0020-7683(97)00120-0

VISCOELASTIC ANALYSIS OF CREEP RESPONSE FOR UNIAXIALLY-COMPRESSED LAMINATES WITH INITIAL DEFLECTION INCLUDING THE EFFECT OF PHYSICAL AGING

NAN-NONG HUANG
Department of Mechanical and Marine Engineering, National Taiwan Ocean University, Keelung, Taiwan, Republic of China
E-mail: b0120@crayel.ntou.edu.tw

(*Received* 22 *May* 1996; *in revised form* 21 *January* 1997)

Abstract—The viscoelastic behavior of simply-supported, cross-ply and angle-ply laminated plates with a physical aging phenomenon is examined. The laminates considered are under uniaxial in-plane compression and have various amplitudes of initial imperfection. The analysis is based on a geometrically nonlinear viscoelastic formulation. The effective time theory is employed to construct the stress–strain relations. By assuming every component of relaxation moduli in each lamina has the same aging shift rate, the analysis is conducted on the effective time scale. The stress function is obtained by solving the compatibility equation by the use of the Laplace transform and a numerical integration scheme. Deflection is calculated from the moment equation by the Galerkin method in conjunction with the numerical integration. Numerical results for deflection history and edge shortening for the glass-reinforced vinyl ester laminates are presented. The effects of the physical aging, the pre-loading aging time, the amplitude of imperfection, the magnitude of loading, and the coupling relaxation moduli on the creep responses are illustrated in the numerical examples. Solutions based on the quasi-elastic approach are also presented for comparison. © 1998 Elsevier Science Ltd.

INTRODUCTION

Although it is well-known that the polymer matrix composite exhibits a viscoelastic behavior, the creep buckling and large creep deflection of fiber-reinforced plastic (FRP) laminates receive little attention. Among a few works on this subject, Wilson and Vinson (1984) investigated the buckling load reduction of the graphite-reinforced epoxy. Kim and Hong (1988) examined the viscoelastic buckling load of sandwich plates with cross-ply faces. Both works are based on the linear buckling analysis. More recently, Huang (1994) has studied the viscoelastic buckling and postbuckling of circular cylindrical laminated shells. These works were conducted within the framework of the quasi-elastic analysis; i.e. the viscoelastic responses are obtained by direct substitution of time-varying properties into the elastic formulations of the problem.

The quasi-elastic approximation ignoring the history of stress resultant variation in a plate is applicable to the case when the internal forces and moments are nearly timewise constant, for example, a plate under a constant transverse loading. However, for the case of a compressed plate, the deflection (or curvature) is induced by the existence of the bending moment, which in turn depends mainly on the magnitude of the deflection. Therefore, the bending moment is time-varying and may change rapidly in the creep process, although the compressive forces along the edges are held constant. Thus, the applicability of the much simpler quasi-elastic approach to the plates under compression appears to be questionable.

Another shortcoming in the above-mentioned works is that the viscoelastic buckling analysis is conducted without considering the effect of initial imperfections. The creep behavior of a viscoelastic plate under compression is characterized by the growth of the initial deflection. It is known that the amplitude of imperfection will affect the time at which the deflection grows rapidly (Boley and Weiner, 1985). Theoretically, a geometrically perfect viscoelastic plate will never deflect if the applied compressive loading does not exceed the instantaneous buckling load.

Shalev and Aboudi (1991) had used the viscoelastic approach to investigate the post-buckling creep behaviors for geometrically perfect, symmetric cross-ply laminates. Trigonomeric functions are employed to represent the displacements, and the approximate solutions are obtained using the Galerkin procedure. Shalev and Aboudi did not consider the cases when the applied load is smaller than the instantaneous buckling load, since the implication of the geometric imperfection is not included in their formulations. Recently, Marques and Creus (1994) have used the viscoelastic approach in conjunction with the finite element method to study the responses of laminated plates and shells to the transverse mechanical loadings and hygrothermal loads. The effect of the imperfection on the creep responses of laminated plates to the in-plane compression are not reported. Therefore, to further clarify the visoelastic behaviors of the FRP laminates under compression, the creep responses of simply-supported FRP laminates having various degrees of imperfections are examined based on the geometrically nonlinear viscoelastic analysis in this study. The laminates considered are symmetric cross-ply and antisymmetric angle-ply laminates.

In addition to the viscoelastic property, the polymeric materials and polymeric composites exhibit a physical aging phenomenon when placed in an environment with temperature between the glass transition temperature and the temperature of the highest secondary transition (Struik, 1978). The influence of physical aging effect on the viscoelastic behavior of polymer matrix composites has been studied extensively in recent years. However, most investigations so far have been devoted to the modeling of viscoelastic properties, which includes the construction of momentary (short-term) master curve for creep compliances and the examination of the validity of the effective time theory. To the author's best knowledge, the analysis of creep responses of laminate structures with physical aging property has not been reported. In this paper, the influence of the physical aging effect on the structural responses is illustrated by examining the creep behaviors of composite plates with imperfections under in-plane compression.

Since the material properties change due to aging, the Boltzmann's superposition principle cannot be directly applied to the viscoelastic material with aging phenomenon. The effective time theory is introduced to construct the stress–strain relation for a lamina. The compatibility and moment equilibrium equations, expressed in the form of convolution integrals, are employed to govern the structural responses. By applying the Laplace transform to the compatibility equation, the Laplace transform of the stress function can be obtained exactly. The stress function obtained from the inverse Laplace transform is accomplished by the assistance of the trapezoid integration rule. The deflection parameter is determined from the moment equation using the Galerkin technique in conjunction with the numerical integration scheme. The creep responses of glass-reinforced bis-phenol A vinyl ester (glass/BPA) laminates are reported. The results based on the quasi-elastic approach are also presented and compared to the viscoelastic solutions to assess the validity of the quasi-elastic analysis.

STRESS–STRAIN RELATION FOR A LAMINA WITH PHYSICAL AGING

The viscoelastic behavior of polymer materials is associated with the mobility of chain segment M. Usually, the mobility diminishes with the elapsed time of aging t_e. According to Struik (1978), the relation between M and t_e is governed by

$$M(t_e) = k/(t_e)^{\mu} \tag{1}$$

where k is a constant and μ is called the aging shift rate.

Generally, the creep behavior of a physical aging material is described by the momentary (or short-term) creep compliances, where it is assumed that no aging occurs during creep. Suppose that the momentary creep compliance of a specially orthotropic lamina with aging time t_e are $S_{ij}(t, t_e)$ $(i, j = 1, 2, 6)$. Then, according to the time/aging-time superposition principle, the momentary creep compliances of the same material with aging time t'_e can be related to $S_{ij}(t, t_e)$ as

$$S_{ij}(t, t'_e) = S_{ij}(a_{ij}(t'_e, t_e)t, t_e) \quad (i,j = 1,2,6) \tag{2}$$

where a_{ij} is called the acceleration factor, which represents the ratio of mobility corresponding to different values of aging time t_e and t'_e. According to eqn (1), the acceleration factor for each component of creep compliance is

$$a_{ij}(t'_e, t_e) = (t_e/t'_e)^{\mu_{ij}} \tag{3}$$

in which μ_{ij} represents the aging shift rate corresponding to each component of S_{ij}.

The long-term creep behavior of a physical aging material is fundamentally different from the short-term creep response to the loading; the creep phenomenon is accompanied by the simultaneous aging. Consider a material with aging time t_e; in the time interval between t and $t+\mathrm{d}t$, the creep response is $1/a_{ij}(t_e+t, t_e)$ times slower than at $t = 0$. Therefore, the interval is equivalent to an effective time interval $\mathrm{d}\lambda_{ij}$ which is given by

$$\mathrm{d}\lambda_{ij}(t, t_e) = a_{ij}(t_e+t, t_e)\,\mathrm{d}t.$$

Based on the above equation, the effective time is

$$\lambda_{ij}(t, t_e) = \int_0^t a_{ij}(t_e+\tau, t_e)\,\mathrm{d}\tau.$$

Introducing eqn (3) and integrating the above equation yields

$$\lambda_{ij}(t, t_e) = t_e \ln(1+t/t_e) \quad \text{if } \mu_{ij} = 1$$

$$\lambda_{ij}(t, t_e) = \frac{t_e}{1-\mu_{ij}}[(1+t/t_e)^{1-\mu_{ij}} - 1] \quad \text{if } \mu_{ij} \neq 1. \tag{4}$$

Therefore, from the meaning of the effective time, the long-term creep compliance of a lamina with aging time t_e are

$$S^{\mathrm{L}}_{ij}(t, t_e) = S_{ij}(\lambda_{ij}(t, t_e), t_e) \quad (i,j = 1,2,6).$$

The Boltzmann's superposition principle is applicable to the short-term viscoelastic response of materials with physical aging. Consequently, the momentary stress–strain relations for a specially orthotropic lamina under a state of plane stress with aging time t_e can be written as follows (Brinson and Gates, 1995)

$$\varepsilon_i(t) = \sum_{j=1,2,6} \int_{-\infty}^{t} S_{ij}(t-\tau)\frac{\partial \sigma_j(\tau)}{\partial \tau}\mathrm{d}\tau \quad (i = 1,2,6) \tag{5a}$$

$$\sigma_i(t) = \sum_{j=1,2,6} \int_{-\infty}^{t} Q_{ij}(t-\tau)\frac{\partial \varepsilon_j(\tau)}{\partial \tau}\mathrm{d}\tau \quad (i = 1,2,6) \tag{5b}$$

where Q_{ij} are the momentary reduced relaxation moduli. Functions σ_i, ε_i, S_{ij} and Q_{ij} are equal to zero when $t < 0$. It is noted that, to make the expression more concise, the reference aging time t_e has been dropped from eqn (5). The same abbreviation is also applied to all the equations appearing hereafter. Applying the Laplace transform to eqn (5) yields the following equations in the transform variable s:

$$\sum_{k=1,2} [\hat{S}_{ik}(s\hat{Q}_{kj})] = \delta_{ij}/s \quad (i,j = 1,2)$$

$$\hat{S}_{66}(s\hat{Q}_{66}) = 1/s$$

where δ_{ij} is the Kronecker delta, and a variable with a hat (^) represents the Laplace transform of this variable. Taking the inverse Laplace transform of the above equations gives the following useful expressions regarding the relations between $S_{ij}(t)$ and $Q_{ij}(t)$:

$$\sum_{k=1,2}\left[\int_0^t S_{ik}(t-\tau)\frac{\mathrm{d}Q_{kj}(\tau)}{\mathrm{d}\tau}\mathrm{d}\tau + S_{ik}(t)Q_{kj}(0)\right] = \delta_{ij} \quad (i,j=1,2) \tag{6a}$$

$$\int_0^t S_{66}(t-\tau)\frac{\mathrm{d}Q_{66}(\tau)}{\mathrm{d}\tau}\mathrm{d}\tau + S_{66}(t)Q_{66}(0) = 1. \tag{6b}$$

The above equations will be used later to calculate $Q_{ij}(t)$ from $S_{ij}(t)$ by employing the numerical integration scheme.

It is known that, due to the change of the material property, the Boltzmann's superposition principle cannot be applied directly to the long-term stress–strain relation. Based on the effective time theory, the long-term strain–stress relation for a lamina with prestraining aging time t_e is as follows:

$$\varepsilon_i(t) = \sum_{j=1,2}\int_{-\infty}^t S_{ij}(\lambda_{ij}(t)-\tilde{\lambda}_{ij}(\tau))\frac{\partial\sigma_j(\tau)}{\partial\tau}\mathrm{d}\tau \quad (i=1,2) \tag{7a}$$

$$\varepsilon_6(t) = \int_{-\infty}^t S_{66}(\lambda_{66}(t)-\tilde{\lambda}_{66}(\tau))\frac{\partial\sigma_6(\tau)}{\partial\tau}\mathrm{d}\tau. \tag{7b}$$

For the case that the lamina whose time-dependent property in S_{11} and S_{12} can be ignored and the case that the lamina exhibits the same aging shift rate for the creep responses to the axial loading (i.e. $\mu_{11} = \mu_{12} = \mu_{22}$), the long-term stress–strain relations can be written as

$$\sigma_i(t) = \sum_{j=1,2}\int_{-\infty}^t Q_{ij}(\lambda_{22}(t)-\tilde{\lambda}_{22}(\tau))\frac{\partial\varepsilon_j(\tau)}{\partial\tau}\mathrm{d}\tau \quad (i=1,2) \tag{8a}$$

$$\sigma_6(t) = \int_{-\infty}^t Q_{66}(\lambda_{66}(t)-\tilde{\lambda}_{66}(\tau))\frac{\partial\varepsilon_6(\tau)}{\partial\tau}\mathrm{d}\tau. \tag{8b}$$

From some types of material systems, the aging shift rate corresponding to the axial and shear creep responses are almost identical (Sullivan *et al.*, 1993). By taking $\mu_{22} = \mu_{66} = \mu$, the long-term stress–strain relations (8) can be expressed as

$$\sigma_i(\lambda(t)) = \sum_{j=1,2,6}\int_{-\infty}^{\lambda} Q_{ij}(\lambda(t)-\tilde{\lambda}(\tau))\frac{\partial\varepsilon_j(\tilde{\lambda})}{\partial\tilde{\lambda}}\mathrm{d}\tilde{\lambda} \equiv \sum_{j=1,2,6} Q_{ij}{}^{*}\varepsilon_j' \quad (i=1,2,6). \tag{9}$$

Hereafter, the asterisk (*) indicates a convolution integral, and the prime (′) denotes the derivative with respect to the effective time. It is noted that the above expression is identical to the expression (5b) regarding the short-term stress–strain relation once the effective time is replaced by the real time. Therefore, the analysis can be conducted on the effective time scale. Once the problem is solved, the results are then transformed back on the real time scale. In this study, the creep analysis of FRP structures is restricted to this type of material system.

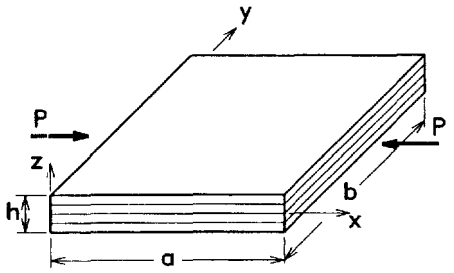

Fig. 1. Laminated plate.

GOVERNING FORMULATIONS FOR A LAMINATE

Consider a composite laminate as shown in Fig. 1. The laminate under consideration consists of N viscoelastic layers, with each layer taken to be macroscopically homogeneous and orthotropic. Each layer is subjected to the same period of pre-loading aging, and every component of the creep compliances has an identical aging shift rate. The edge widths of the plate in the x- and y-directions are denoted as a and b, respectively and the thickness is h. The plate considered, having an initial deflection w_0, carries an in-plane compressive force P along the x-direction.

According to the classical plate theory and von Kármán flexible plate assumption, the strains ε_i^0 and curvatures κ_i of the middle plane are related to the displacements by (Uemura and Byon, 1977)

$$\begin{aligned}
\varepsilon_x^0 &= u_{,x} + (w_{,x})^2/2 + w_{,x}w_{0,x} \\
\varepsilon_y^0 &= v_{,y} + (w_{,y})^2/2 + w_{,y}w_{0,y} \\
\gamma_{xy}^0 &= v_{,x} + u_{,y} + w_{,x}w_{,y} + w_{,x}w_{0,y} + w_{0,x}w_{,y} \\
\kappa_x &= -w_{,xx}, \quad \kappa_y = -w_{,yy}, \quad \kappa_{xy} = -2w_{,xy}
\end{aligned} \tag{10}$$

where u and v are displacements of the middle plane in the x- and y-directions, respectively; w is the induced deflection after loading is applied.

Consider symmetric cross-ply and antisymmetric angle-ply laminates. The stress resultants can be related with strains and curvatures as

$$N_i = \sum_{j=1,2,6} [A_{ij}*(\varepsilon_j^0)' + B_{ij}*\kappa_j'] \quad (i = 1,2,6) \tag{11}$$

$$M_i = \sum_{j=1,2,6} [B_{ij}*(\varepsilon_j^0)' + D_{ij}*\kappa_j'] \quad (i = 1,2,6) \tag{12}$$

where $A_{16} = A_{26} = D_{16} = D_{26} = 0$ and $B_{11} = B_{12} = B_{22} = B_{66} = 0$. For the case of symmetric cross-ply laminates, components B_{16} and B_{26} also vanish. The effective relaxation moduli A_{ij}, B_{ij} and D_{ij} listed in eqns (11) and (12) are defined by

$$(A_{ij}, B_{ij}, D_{ij}) = \sum_{k=1}^{N} \int (1, z, z^2)(\bar{Q}_{ij})_k \, dz \quad (i,j = 1,2,6)$$

in which $(\bar{Q}_{ij})_k$ are the transformed reduced relaxation moduli of the kth layer, which can be calculated from the reduced relaxation moduli $(Q_{ij})_k$ using the tensor component transformation. Taking the Laplace transform of eqn (11), the following equations are obtained:

$$\hat{\varepsilon}_i^0 = \sum_{j=1,2,6} \left(\frac{1}{s} a_{ij} \hat{N}_j + b_{ij} \hat{\kappa}_j \right) \quad (i = 1, 2, 6) \tag{13}$$

where

$$[a] = [\hat{A}]^{-1} \quad [b] = -[a][\hat{B}].$$

The quasi-static analysis is employed in this study. The in-plane gross equilibrium equations are

$$N_{x,x} + N_{xy,y} = 0 \quad N_{xy,x} + N_{y,y} = 0 \tag{14}$$

and the out-of-plane response is governed by

$$M_{x,xx} + 2M_{xy,xy} + M_{y,yy} + N_x(w+w_0)_{,xx} + 2N_{xy}(w+w_0)_{,xy} + N_y(w+w_0)_{,yy} = 0. \tag{15}$$

Let the stress function F be defined by

$$N_x = F_{,yy} \quad N_y = F_{,xx} \quad N_{xy} = -F_{,xy}. \tag{16}$$

The force resultants N_x, N_y and N_{xy} thus related to the stress function F satisfy the in-plane force equilibrium equations (14). Upon introducing the stress function and eqns (10) and (12) into (15), the moment equation is rewritten as below

$$\begin{aligned}
&D_{11}{}^* w'_{,xxxx} + 2(D_{12} + 2D_{66})^* w'_{,xxyy} + D_{22}{}^* w'_{,yyyy} \\
&- 3B_{16}{}^* u'_{,xxy} - B_{26}{}^* u'_{,yyy} - 3B_{26}{}^* v'_{,xyy} - B_{16}{}^* v'_{,xxx} \\
&- 2B_{16}{}^* (w_{,x} w_{,x}/2 + w_{,x} w_{0,x})'_{,xy} - B_{16}{}^* (w_{,x} w_{,y} + w_{,x} w_{0,y} + w_{0,x} w_{,y})'_{,xx} \\
&- 2B_{26}{}^* (w_{,y} w_{,y}/2 + w_{,y} w_{0,y})'_{,xy} - B_{26}{}^* (w_{,x} w_{,y} + w_{,x} w_{0,y} + w_{0,x} w_{,y})'_{,yy} \\
&- F_{,yy}(w+w_0)_{,xx} + 2F_{,xy}(w+w_0)_{,xy} - F_{,xx}(w+w_0)_{,yy} = 0.
\end{aligned} \tag{17}$$

The compatibility condition for a physically possible strain state, obtained from eqn (10), is as follows,

$$\varepsilon^0_{x,yy} + \varepsilon^0_{y,xx} - \gamma^0_{xy,xy} = (w_{,xy})^2 - w_{,xx} w_{,yy} + 2w_{,xy} w_{0,xy} - w_{,xx} w_{0,yy} - w_{0,xx} w_{,yy}. \tag{18}$$

By applying the Laplace transform to the above equation and introducing eqns (13) and (16), the compatibility equation can be expressed as

$$\begin{aligned}
&a_{22} \hat{F}_{,xxxx} + (2a_{12} + a_{66}) \hat{F}_{,xxyy} + a_{11} \hat{F}_{,yyyy} \\
&= s\mathcal{L}[(w_{,xy})^2 - w_{,xx} w_{,yy} + 2w_{,xy} w_{0,xy} - w_{,xx} w_{0,yy} - w_{0,xx} w_{,yy}] \\
&\quad + s(2b_{26} - b_{61}) \hat{w}_{,xxxy} + s(2b_{16} - b_{62}) \hat{w}_{,xyyy}.
\end{aligned} \tag{19}$$

Here, the symbol ($\mathcal{L}$) represents the Laplace transform.

VISCOELASTIC ANALYSIS

The viscoelastic responses of simply-supported composite laminates under in-plane compression are analyzed. The specific boundary conditions along the edges are

$$\text{at } x = 0, a: w = M_x = N_{xy} = 0, \quad u = \text{constant} \quad \text{and} \quad \int_0^b N_x \, dy = -PH(t)$$

$$\text{at } y = 0, b: w = M_y = N_{xy} = 0, \quad v = \text{constant} \quad \text{and} \quad \int_0^a N_y \, dx = 0 \tag{20}$$

where $H(t)$ is the Heaviside unit function.

The initial deflection w_0 and the induced deflection after loading w are expressed as

$$[w_0, w] = [A_0, A(t)] \sin(\alpha_m x) \sin(\beta_n y)$$

where $\alpha_m = m\pi/a$ and $\beta_n = n\pi/b$. The deflection pattern $\sin(\alpha_m x) \sin(\beta_n y)$ is chosen to be the same as the instantaneous buckling shape. Here, only one mode is employed to approximate the deflection. For a plate under axial compression, a one-mode approximation generally yields acceptable results for moderately large deflections (Timoshenko and Gere, 1961).

For the assumed deflection w and the prescribed imperfection w_0, the Laplace transform ($\bar{F}$) of the stress function can be determined from eqn (19). By performing the inverse Laplace transform, the stress function F is obtained as follows:

$$F(x, y, \lambda) = \frac{h^3}{32}[(\phi_{11}/\eta^2)\cos(2\beta_n y) + \phi_{22}\eta^2 \cos(2\alpha_m x)]*(\bar{A}^2 + 2\bar{A}_0\bar{A})' - \frac{PH}{2b}y^2$$
$$- h^3\phi_{55}*(\bar{A})' \cos(\alpha_m x)\cos(\beta_n y) \tag{21}$$

where

$$\eta = \beta_n/\alpha_m \quad \bar{A} = A/h \quad \bar{A}_0 = A_0/h$$
$$\phi_{55} = \mathscr{L}^{-1}\left(\frac{G(s)}{h^2}\right) \quad G(s) = \frac{(2b_{16} - b_{62})\eta^3 + (2b_{26} - b_{61})\eta}{a_{22} + (2a_{12} + a_{66})\eta^2 + a_{11}\eta^4}$$
$$\phi_{11} = \mathscr{L}^{-1}\left(\frac{1}{a_{11}h}\right) \quad \phi_{22} = \mathscr{L}^{-1}\left(\frac{1}{a_{22}h}\right). \tag{22}$$

The operator ($\mathscr{L}^{-1}$) appearing in the above formulations represents the inverse Laplace transform. The resultant forces N_x, N_y and N_{xy} can be easily determined from eqn (16); the explicit expressions for the forces will not be provided here. It is not difficult to verify that the stress function F given in eqn (21) satisfies the force boundary conditions listed in (20).

It is generally very difficult to obtain functions ϕ_{11}, ϕ_{22} and ϕ_{55} from eqn (22) by performing the inverse Laplace transform. Here, the values of these functions are evaluated using a numerical integration scheme. It can be shown that functions ϕ_{11}, ϕ_{22} and ϕ_{55} satisfy the following relations:

$$(A_{22}/h)*\phi'_{11} = f_1, \quad (A_{11}/h)*\phi'_{22} = f_1$$
$$\phi_{67}*\phi'_{55} = \eta^3[f_2*(A'_{66}/h) + f_1*(B'_{26}/h^2)] + \eta[f_3*(A'_{66}/h) + f_1*(B'_{16}/h^2)] \tag{23}$$

where

$$f_1 = (A_{11}*A'_{22} - A_{12}*A'_{12})/h^2 \quad f_2 = 2(A_{12}*B'_{26} - A_{22}*B'_{16})/h^3$$
$$f_3 = 2(A_{12}*B'_{16} - A_{11}*B'_{26})/h^3 \quad \phi_{67} = C_{11}*C'_{22} - C_{12}*C'_{21}$$
$$C_{11} = (A_{11} + \eta^2 A_{66})/h \quad C_{22} = (\eta^2 A_{22} + A_{66})/h$$
$$C_{21} = (A_{12} + A_{66})/h \quad C_{12} = \eta^2 C_{21}. \tag{24}$$

The convolution integrals appearing in eqns (23) and (24) are integrated using the trapezoid integration rule. Here, for the purpose of illustration, the numerical integration scheme for $A_{22}*\phi'_{11}$ is presented. First, it is appropriate to express $A_{22}*\phi'_{11}$ as follows (Christensen, 1982):

$$A_{22}*\phi'_{11} = A_{22}(\lambda)\phi_{11}(0)+\int_0^{\lambda} A_{22}(\lambda-\tilde{\lambda})\frac{\mathrm{d}\phi_{11}(\tilde{\lambda})}{\mathrm{d}\tilde{\lambda}}\mathrm{d}\tilde{\lambda}.$$

Consider the integration value of $A_{22}*\phi'_{11}$ from $\lambda = 0$ to $\lambda = \lambda_j$ to be calculated. According to the trapezoid rule, the following numerical formulation can be obtained:

$$\begin{aligned} A_{22}*\phi'_{11} &= A_{22}(\lambda_j)\phi_{11}(0)+\int_0^{\lambda_j} A_{22}(\lambda_j-\tilde{\lambda})\frac{\mathrm{d}\phi_{11}(\tilde{\lambda})}{\mathrm{d}\tilde{\lambda}}\mathrm{d}\tilde{\lambda} \\ &\approx A_{22}(\lambda_j)\phi_{11}(0) \\ &\quad +\sum_{k=0}^{j-1}\frac{1}{2}[A_{22}(\lambda_j-\lambda_k)+A_{22}(\lambda_j-\lambda_{k+1})][\phi_{11}(\lambda_{k+1})-\phi_{11}(\lambda_k)] \end{aligned} \tag{25}$$

where λ_k $(k = 0, 1, 2, \ldots, j)$ $(\lambda_0 = 0)$ are the effective time intervals.

Here, the procedure of numerical calculation of ϕ_{11} is briefly illustrated. Suppose that the values of $\phi_{11}(\lambda_k)$ $(k = 0, 1, 2, \ldots, j-1)$ have been determined. Evaluating the convolution integrals in eqns (23) and (24) according to the above numerical formulation (25) generates an algebraic equation for $\phi_{11}(\lambda_j)$. Therefore, the value of ϕ_{11} at effective time $\lambda = \lambda_j$ can be decided. The same procedure is repeated to calculate the value of ϕ_{11} at time $\lambda = \lambda_{j+1}$, and so on for the successive time intervals.

The in-plane displacements u and v can be determined from the following strain-force relations:

$$\hat{\varepsilon}_x^0 = (a_{11}\hat{N}_x+a_{12}\hat{N}_y)/s+b_{16}\hat{\kappa}_{xy} \quad \hat{\varepsilon}_y^0 = (a_{12}\hat{N}+a_{22}\hat{N}_y)/s+b_{26}\hat{\kappa}_{xy}.$$

Upon introducing stress function (16) and employing strain–displacement relations (10), the above expressions become

$$\begin{aligned} \hat{u}_{,x} &= (a_{11}\hat{F}_{,yy}+a_{12}\hat{F}_{,xx})/s-2b_{16}\hat{w}_{,xy}-\mathscr{L}(w_{,x}^2/2+w_{,x}w_{0,x}) \\ \hat{v}_{,y} &= (a_{12}\hat{F}_{,yy}+a_{22}\hat{F}_{,xx})/s-2b_{26}\hat{w}_{,xy}-\mathscr{L}(w_{,y}^2/2+w_{,y}w_{0,y}). \end{aligned}$$

Integrating the above equations and performing the inversion of the Laplace transforms yields

$$\begin{aligned} u(x,y,\lambda)/a = &-\frac{1}{8}(\alpha_m h)^2(\bar{A}^2+2\bar{A}_0\bar{A})\left[\frac{x}{a}+\frac{1}{\alpha_m a}\sin^2(\beta_n y)\sin(2\alpha_m x)\right] \\ &-\frac{1}{16\alpha_m a}(\beta_n h)^2\phi_{33}*(\bar{A}^2+2\bar{A}_0\bar{A})'\sin(2\alpha_m x)-\frac{P}{bh}\frac{x}{a}\psi_{11}+\frac{(\alpha_m h)^2}{\alpha_m a}\phi_{66}*\bar{A}'\sin(\alpha_m x)\cos(\beta_n y) \end{aligned} \tag{26}$$

$$\begin{aligned} v(x,y,\lambda)/b = &-\frac{1}{8}(\beta_n h)^2(\bar{A}^2+2\bar{A}_0\bar{A})\left[\frac{y}{b}+\frac{1}{\beta_n b}\sin^2(\alpha_m x)\sin(2\beta_n y)\right] \\ &-\frac{1}{16\beta_n b}(\alpha_m h)^2\phi_{44}*(\bar{A}^2+2\bar{A}_0\bar{A})'\sin(2\beta_n y)-\frac{P}{bh}\frac{y}{b}\psi_{12}+\frac{(\beta_n h)^2}{\beta_n b}\phi_{77}*\bar{A},\cos(\alpha_m x)\sin(\beta_n y) \end{aligned} \tag{27}$$

with

$$\phi_{33} = \mathscr{L}^{-1}\left(\frac{a_{12}}{sa_{22}}\right) \quad \psi_{11} = \mathscr{L}^{-1}\left(\frac{ha_{11}}{s^2}\right) \quad \phi_{44} = \mathscr{L}^{-1}\left(\frac{a_{12}}{sa_{11}}\right) \quad \psi_{12} = \mathscr{L}^{-1}\left(\frac{ha_{12}}{s^2}\right)$$

$$\phi_{66} = \mathscr{L}^{-1}\left\{\frac{a_{11}G(s)\eta^2 + a_{12}G(s) - 2\eta b_{16}}{hs}\right\}$$

$$\phi_{77} = \mathscr{L}^{-1}\left\{\frac{a_{12}G(s) + a_{22}G(s)/\eta^2 - 2b_{26}/\eta}{hs}\right\}. \tag{28}$$

The displacements in eqns (26) and (27) are determined by imposing normal in-plane displacement $u(0, y, \lambda) = v(x, 0, \lambda) = 0$. It is noted that the displacements listed in eqns (26) and (27) satisfy in-plane movement requirements along the edges $x = a$ and $y = b$. Also, the resulting internal moments calculated from eqns (12) also meet the boundary moment requirements. The edge shortening δ along the x direction is given by

$$\delta/a = -u(x = a, y, \lambda)/a = (\alpha_m h)^2(\bar{A}^2 + 2\bar{A}_0\bar{A})/8 + (P/bh)\psi_{11}. \tag{29}$$

The values of functions ϕ_{33}, ϕ_{44}, ϕ_{66}, ϕ_{77}, ψ_{11} and ψ_{12} appearing in eqn (28) are calculated numerically. It can be shown that these functions satisfy the following relations:

$$A_{11}{}^*\phi'_{33} = -A_{12} \quad A_{22}{}^*\phi'_{44} = -A_{12}\phi_{11}{}^*\psi'_{11} = 1 \quad \phi_{11}{}^*\psi'_{12} = \phi_{44}$$
$$\phi_{67}{}^*\phi'_{66} = b_1{}^*C'_{22} - B_2{}^*C'_{12} \quad \phi_{67}{}^*\phi'_{77} = B_2{}^*C'_{11} - b_1{}^*C'_{21} \tag{30}$$

where

$$b_1 = \eta^2 B_1 \quad B_1 = (3B_{16} + \eta^2 B_{26})/h^2 \quad B_2 = (B_{16} + 3\eta^2 B_{26})/h^2 \tag{31}$$

and C_{11}, C_{12}, C_{21}, C_{22} and ϕ_{67} are given in eqn (24). The values of these functions at a specific time $\lambda = \lambda_j$ can be determined by evaluating all the convolution integrals in eqn (30) according to the numerical formulation (25) and following the afore-mentioned procedure.

Next, the expressions for displacements u and v, deflections w and w_0, and stress function F are substituted into the moment equation (17). The equation will not be satisfied exactly, but will have a residual R (say) owing to the approximate nature of w. The Galerkin method is employed here which requires

$$\int_0^b \int_0^a R \sin(\alpha_m x) \sin(\beta_n y)\, dx\, dy = 0.$$

Substituting expression (17) into the above equation and performing the integration yields the following nonlinear equation:

$$-(P/P_{cr})[D(0) - B(0)](\bar{A}_0 + \bar{A}) + [D(\lambda) - B(\lambda)]{}^*\bar{A} + (\bar{A}_0 + \bar{A})[\phi^*(2\bar{A}_0\bar{A} + \bar{A}^2)']/16 = 0 \tag{32}$$

where

$$\phi = \phi_{11} + \eta^4\phi_{22} \quad D(\lambda) = [D_{11} + 2\eta^2(D_{12} + 2D_{66}) + \eta^4 D_{22}]/h^3$$
$$B(\lambda) = \eta[B_1{}^*(\phi_{66})' + B_2{}^*(\phi_{77})'] \quad P_{cr} = (\alpha_m)^2 bh^3[D(0) - B(0)]. \tag{33}$$

The commutative and associative laws of convolution integrals (Christensen, 1982) have been employed to derive eqns (32) and (33). It is unlikely to solve eqn (32) exactly. The trapezoid integration rule is employed to obtain approximate solutions for the unknown

deflection parameter $\bar{A}$. Evaluating all the convolution integrals in eqns (32) and (33) according to the numerical formulation (25) yields a cubic equation for $\bar{A}(\lambda_j)$. Therefore, the deflection magnitude at effective time $\lambda = \lambda_j$ can be easily determined.

Parameter P_{cr} in eqn (33) represents the instantaneous buckling load which is identical to the elastic buckling load of a laminate whose viscoelastic effect is ignored. With definitions of P_{cr} and $D(\lambda)$, the edge shortening expression (29) can be rewritten as

$$\bar{\delta} = (\delta/a)/(\alpha_m h)^2 = (\bar{A}^2 + 2\bar{A}_0\bar{A})/8 + (P/P_{cr})[D(0) - B(0)]\psi_{11}. \tag{34}$$

Finally, the quasi-elastic approximation for deflection amplitude $\bar{A}$ can be accomplished by replacing the convolution integrals in eqns (32) and (33) with the conventional products; that is

$$-(P/P_{cr})[D(0) - B(0)](\bar{A}_0 + \bar{A}) + [D(\lambda) - B(\lambda)]\bar{A} + (\bar{A}_0 + \bar{A})(2\bar{A}_0\bar{A} + \bar{A}^2)\phi/16 = 0. \tag{35}$$

The material properties are calculated according to the elastic relations, for example

$$[Q] = [S]^{-1} \quad \phi_{11} = 1/\psi_{11} = (A_{11}A_{22} - A_{12}^2)/(A_{22}h).$$

The so-called viscoelastic buckling load, based on the quasi-elastic approach and linear classical buckling analysis, can be determined from eqn (35) by neglecting the nonlinear terms in $\bar{A}$ and without considering the imperfection $\bar{A}_0$. The critical value designated as P_v is given by

$$P_v = (\alpha_m)^2 bh^3[D(\lambda) - B(\lambda)]. \tag{36}$$

The ratio P_v/P_{cr} ($= [D(\lambda) - B(\lambda)]/[D(0) - B(0)]$) is referred to as the buckling load reduction. The controversy over the quasi-elastic analysis has been discussed in the introduction. The validity of quasi-elastic approach will be further assessed using the viscoelastic results in the next section.

NUMERICAL RESULTS AND DISCUSSIONS

The creep responses of glass-reinforced bis-phenol A vinyl ester (glass/BPA) laminates are examined. The momentary master curves for creep compliances S_{ij} of a unidirectional glass/BPA lamina at reference age time $t_e = 70$ h, measured at temperature $T = 60°C$, were given by Sullivan *et al.* (1993). Here, a three-parameter model is employed to describe S_{ij} as follows:

$$\log(S_{ij}/J_r) = b_{ij} + c_{ij}[\log(t/t_r + 1)]^{d_{ij}} \quad J_r = 1/\text{GPa} \quad t_r = 1\text{ s}$$
$$b_{11} = -1.03 \quad b_{22} = -0.881 \quad b_{66} = -0.430$$
$$c_{11} = 0.000532 \quad c_{22} = 0.000277 \quad c_{66} = 0.000344$$
$$d_{11} = 2.98 \quad d_{22} = 3.88 \quad d_{66} = 3.91 \tag{37}$$

where (log) is the common logarithm. The aging shift rate for S_{11}, S_{22} and S_{66} is

$$\mu = 0.75.$$

Sullivan *et al.* did not report the compliance data for S_{12}. Here, a time-invariant Poisson's ratio $\nu_{12} = 0.3$ is assumed for this lamina; that is

$$S_{12} = -0.3S_{11} \tag{38}$$

and the aging shift rate for component S_{12} is also taken to be 0.75. The reduced relaxation moduli Q_{ij} are related to S_{ij} by eqns (6). The values of Q_{ij} can be determined by invoking the numerical integration scheme (25).

The creep deflections and edge shortenings of cross-ply and angle-ply glass/BPA laminates, predicted based on the viscoelastic analysis and quasi-elastic approximation, are presented below. The effects of the physical aging, the pre-loading aging time, the amplitude of initial imperfection, the magnitude of loading, and the number of layers on the viscoelastic behaviors of laminates are demonstrated in the numerical examples. Since the aging shift rate is identical for each component of compliances, the analyses are conducted on the effective time scale. Once the problem is solved, the results are then transformed back on the real time scale according to eqn (4). The results presented in this paper are on the real time scale. The laminates considered hereafter have a buckling mode parameter $\eta = 1$. The laminates are aged and operating in an environment with temperature $T = 60°C$. The pre-loading aging time of the laminates is $t_e = 70$ h, unless special values are indicated elsewhere. The numerical integration for the convolution integrals is based on the equal effective time step.

Creep responses of eight-layer symmetric cross-ply laminates $[(0°/90°)_2]_s$

First, the convergence of numerical results is studied. Consider a laminate with imperfection $\bar{A}_0 = 0.001$ under a compressive loading $P/P_{cr} = 0.8$. The predicted deflections according to various effective time steps $\Delta\lambda = 62{,}500$, 12,500, 2500 and 500 s are plotted against real time in Fig. 2. It is noted that the convergence rate is fast; the solutions corresponding to $\Delta\lambda = 2500$ and 500 s are almost identical. The convergence of all the cases presented hereafter has been thoroughly examined.

Next, consider a laminate with $\bar{A}_0 = 0.01$ subjected to a compressive loading $P/P_{cr} = 0.6$. The deflection histories based on the viscoelastic analysis are shown in Fig. 3. The momentary creep results, obtained by ignoring the physical aging effect, are also included in this figure for comparison. It is seen that the momentary creep deflection deviates sharply from the long-term creep deflection when the time duration exceeds approximately the pre-loading aging time ($t_e = 70$ h). Therefore, the creep deflection of an aging material in a long-term service will be overestimated if the physical aging effect is overlooked.

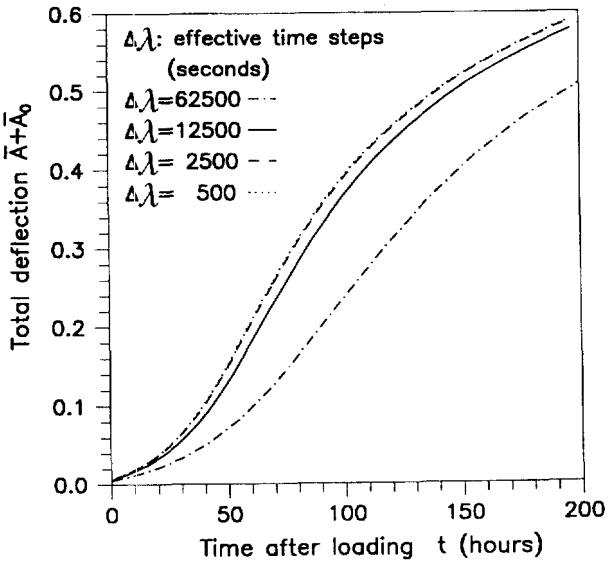

Fig. 2. Deflection histories of a cross-ply laminate according to various effective time steps: ($P/P_{cr} = 0.8, \bar{A}_0 = 0.001, \eta = 1.0, t_e = 70$ h).

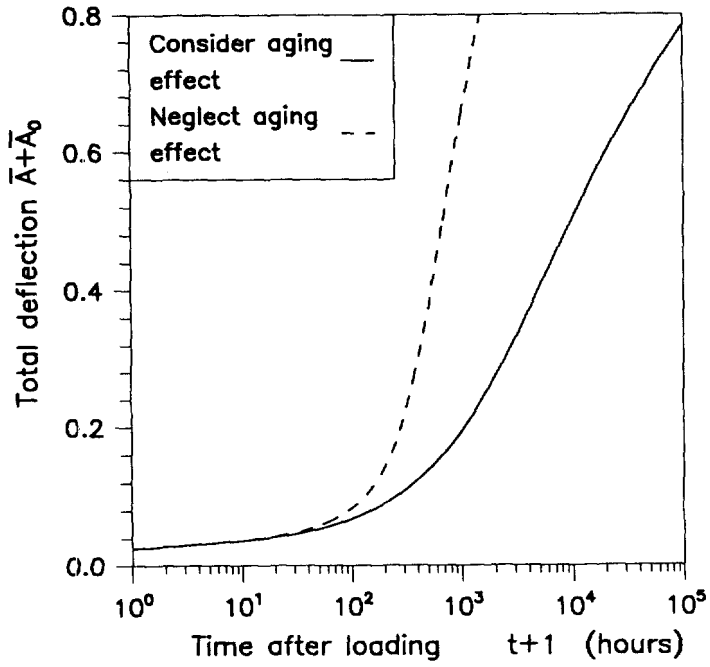

Fig. 3. Momentary and long-term creep deflection histories of a cross-ply laminate: ($P/P_{cr} = 0.6$, $\bar{A}_0 = 0.01, \eta = 1.0, t_e = 70$ h).

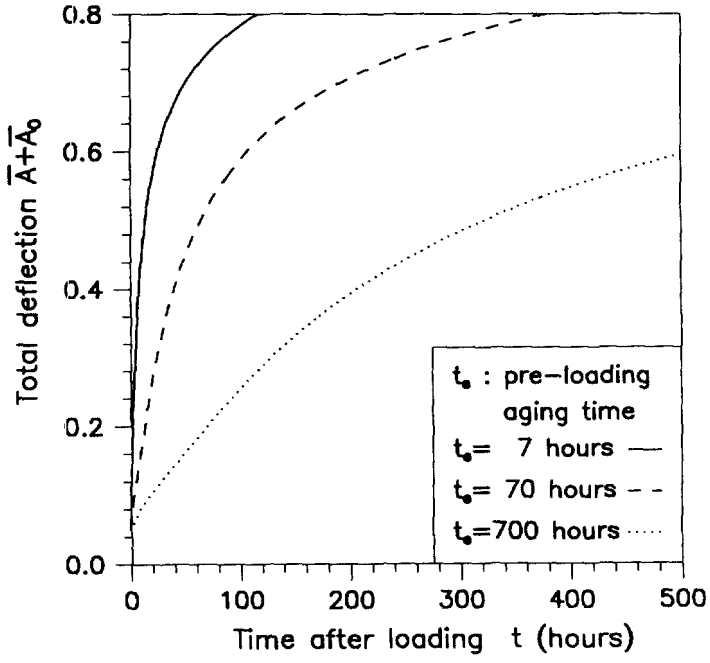

Fig. 4. Deflection histories of cross-ply laminates with various values of pre-loading aging time: ($P/P_{cr} = 0.8, \bar{A}_0 = 0.01, \eta = 1.0$).

Figure 4 depicts the deflection histories of the laminates with $\bar{A}_0 = 0.01$ and $P/P_{cr} = 0.8$, having various values of pre-loading aging time $t = 7$, 70 and 700 h. First, the compliance data listed in eqns (37) and (38) need to be shifted by following the time/aging time superposition principle [eqn (2)]. The results shown in Fig. 4 are based on the viscoelastic analysis. It is noted that a laminate creeps much slower when subjected to a longer period of aging. The results are as expected, since physical aging will reduce the mobility of chain segment and slow down the process of creep.

The deflection histories of laminates under a compressive force $P/P_{cr} = 0.8$, having various amplitudes of initial imperfection $\bar{A}_0 = 0.1$, 0.01, 0.001 and 0.0001, are shown in

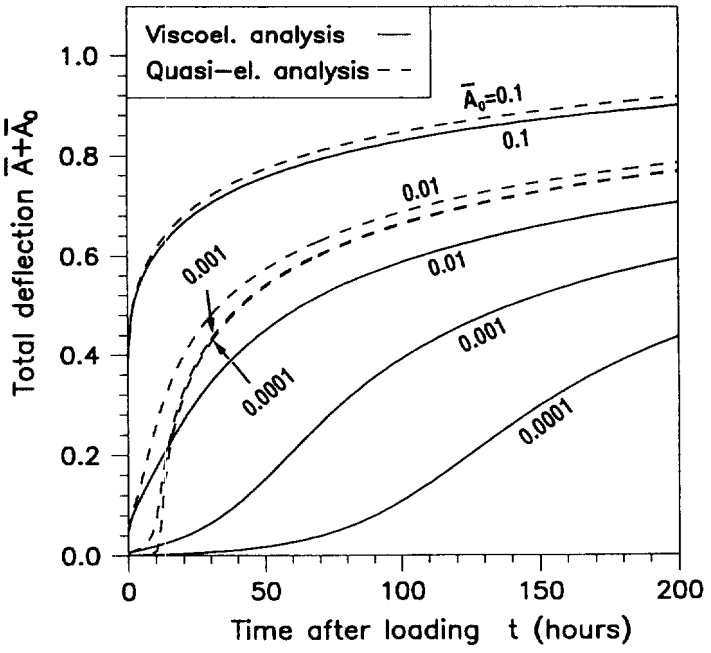

Fig. 5. Deflection histories of cross-ply laminates with various amplitudes of initial imperfection: ($P/P_{cr} = 0.8, \eta = 1.0, t_e = 70$ h).

Fig. 5. Results based on both viscoelastic analysis and quasi-elastic analysis are shown in this figure. For a laminate with a large initial deflection, for example $\bar{A}_0 = 0.1$, the quasi-elastic solutions are in good agreement with the viscoelastic solutions. An explanation for this phenomenon is given below. Note from Fig. 5 that the instantaneous deflection of the laminate with $\bar{A}_0 = 0.1$ is very large, which in turn will induce large values of instantaneous stress resultants. Since the creep behavior of the polymer matrix composites is dominated by the primary stage, it is seen that the laminate creeps rapidly from the onset of the loading, but gradually flattens out. Therefore, most of the changes in stress resultants take place on the very early stage of time duration, which implies that the variation of the stress resultants is moderate. Consequently, the quasi-elastic approximation is applicable to the case when a laminate has a large amplitude of imperfection. However, the deviations between the quasi-elastic and viscoelastic solutions become larger for the cases of laminates having smaller imperfections. The quasi-elastic approach generally predicts a faster growth in creep deflection. For these cases, the instantaneous deflection is seen to be relatively small, which implies that the induced resultant moments are also small at the beginning of the loading. Because the viscoelastic model follows the hereditary law and respects the history of the loading, therefore, the laminate will creep very slowly. Nonetheless, the quasi-elastic model takes the current values of stress resultants to be the constant loads for the whole loading history; consequently, the creep deflection response to the loading predicted by the quasi-elastic analysis is greatly exaggerated.

A further examination of Fig. 5 reveals that for a laminate with a small imperfection, the quasi-elastic analysis predicts a buckling phenomenon occurring at a time approximately 11 h after the load is applied. In other words, the viscoelastic buckling load (P_v) reduces to the 85% of the instantaneous buckling load (P_{cr}) when the laminate sustains a loading for approximately 11 h. However, the more realistic viscoelastic analysis indicates that the laminate undergoes a gradual transition from the regime of small deflection to the regime of large deflection. The transition is not rapid enough to be characterized as a buckling phenomenon. Also, according to the viscoelastic analysis, the deflection history is strongly influenced by the amplitudes of initial imperfection. For example, for a laminate with very small amplitude of imperfection ($\bar{A}_0 = 0.0001$), the laminate sustains a loading duration of 100 hours without yielding a significant deflection. Based on the above observations, the

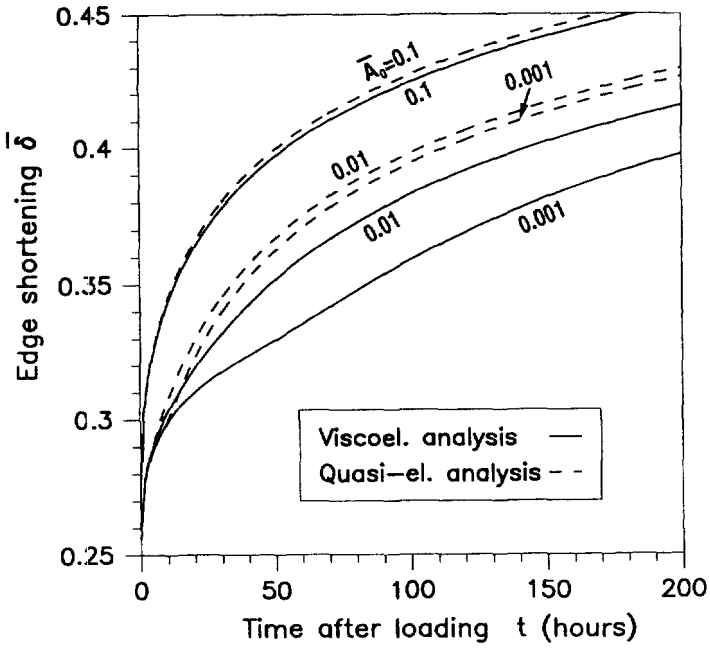

Fig. 6. Edge shortenings of cross-ply laminates with various amplitudes of initial imperfection: ($P/P_{cr} = 0.8, \eta = 1.0, t_c = 70$ h).

validity of viscoelastic buckling predicted using the quasi-elastic approach is seen to be questionable.

Figure 6 shows the edge shortenings of the same laminates considered in the aforementioned example ($P/P_{cr} = 0.8$). Results based on both analyses are shown in the figure for comparison. Again, it is noted that the quasi-elastic analysis is applicable to the cases when laminates have a large imperfection. However, the quasi-elastic approximation cannot produce adequately accurate results of edge shortening for laminates having small imperfections.

Figure 7 shows the deflection histories of a perfect laminate and a laminate with imperfection $\bar{A}_0 = 0.1$, both under a compressive force $P/P_{cr} = 1.05$. Results based on the viscoelastic and quasi-elastic analyses are presented. For both two cases with the compressive load exceeding the instantaneous buckling load P_{cr}, the instantaneous deflections are very large, and the quasi-elastic analysis predicts deflection histories which are very close to those based on the viscoelastic analysis. The nature of the deflection history is similar to the case of a laminate with a large imperfection $\bar{A}_0 = 0.1$ under $P/P_{cr} = 0.8$ as depicted in Fig. 5. It is also seen that the quasi-elastic solutions for the imperfect laminate, which has a larger instantaneous deflection than a perfect laminate, are almost identical to the viscoelastic solutions.

The deflection histories of laminates with imperfection $\bar{A}_0 = 0.01$, under various loadings $P/P_{cr} = 0.8$, 0.7, 0.6 and 0.5, are shown in Fig. 8. The real time coordinate (abscissa) is plotted on the log scale. It is noted that the deflection history is strongly sensitive to the magnitude of loading. The creep rate of deflection for a laminate under a smaller loading is much slower than the creep rate of the same laminate subjected to a larger loading. For a laminate under $P/P_{cr} = 0.6$, it takes more than 100,000 h for the laminate to yield a deflection with an amplitude $\bar{A} = 0.8$; meanwhile, for the same laminate under $P/P_{cr} = 0.8$, the laminate creeps to the same magnitude of deflection within 400 h of loading.

Creep deflections of antisymmetric angle-ply laminates $(-45°/45°)_{N/2}$:

The deflection histories of eight-layer ($N = 8$) laminates under $P/P_{cr} = 0.8$, having various degrees of initial deflection $\bar{A}_0 = 0.1$, 0.01 and 0.0001, are plotted against time duration in Fig. 9. Results based on both viscoelastic and quasi-elastic analyses are reported. For a laminate with a large imperfection ($\bar{A}_0 = 0.1$), the quasi-elastic approximation gives

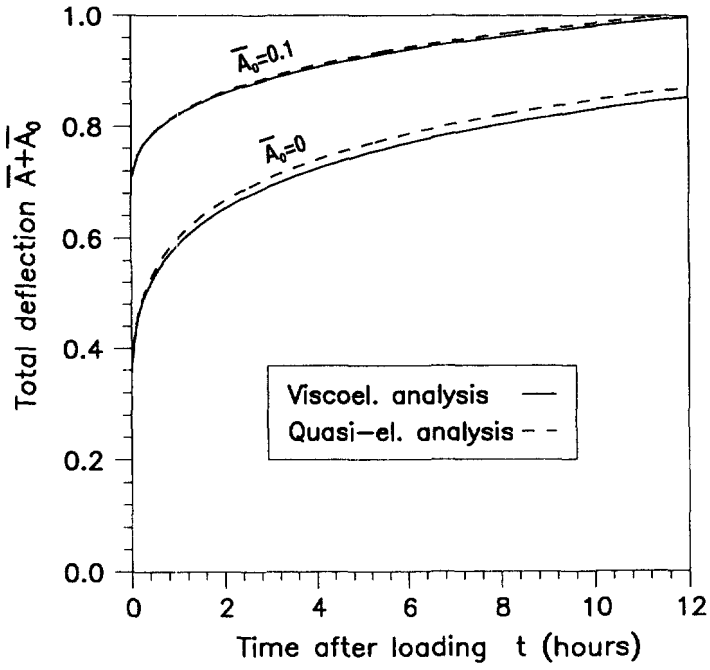

Fig. 7. Deflection histories of cross-ply laminates carrying a load larger than the instantaneous buckling load: ($P/P_{cr} = 1.05, \eta = 1.0, t_e = 70$ h).

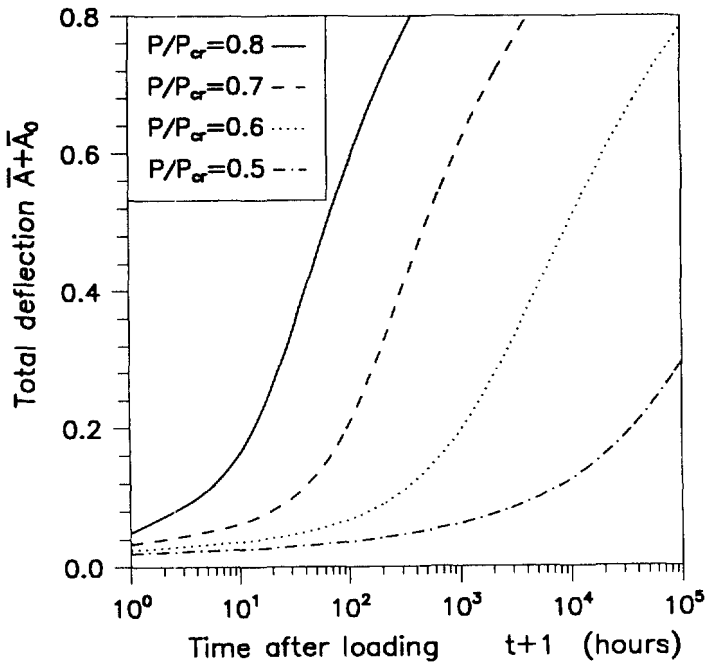

Fig. 8. Deflection histories of cross-ply laminates with various magnitudes of loading: ($\bar{A}_0 = 0.01, \eta = 1.0, t_e = 70$ h).

the results which are very close to the viscoelastic solutions. However, large discrepancies between results based on different approaches are observed for laminates with small imperfections. The quasi-elastic analysis predicts a critical time for buckling at approximately 22 h after loading, which is unlikely to be true as compared to the results based on the more realistic viscoelastic analysis.

Figure 10 depicts the deflection histories of antisymmetric laminates with $\bar{A}_0 = 0.01$ and $P/P_{cr} = 0.8$. The laminates considered have an identical thickness, but consist of different numbers of layers $N = 2$, 4, 8 and ∞. The extensional and bending relaxation

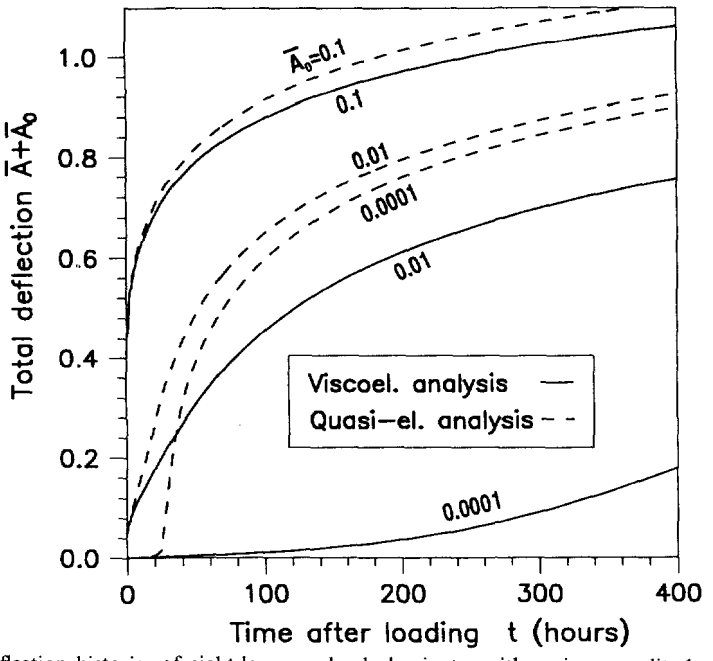

Fig. 9. Deflection histories of eight-layer angle-ply laminates with various amplitudes of initial imperfection: ($P/P_{cr} = 0.8, \eta = 1.0, t_e = 70$ h).

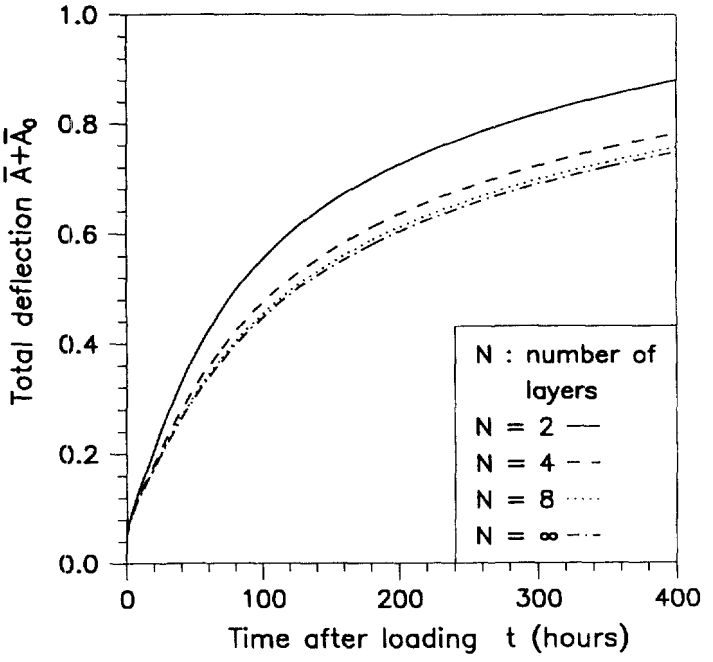

Fig. 10. Deflection histories of angle-ply laminates with various numbers of layers: ($P/P_{cr} = 0.8$, $\bar{A}_0 = 0.01, \eta = 1.0, t_e = 70$ h).

moduli A_{ij} and D_{ij} are identical for laminates having various numbers of layers. Meanwhile, the values of coupling relaxation moduli B_{16} and B_{26} are inversely proportional to the layer number. Letting B_{16} and B_{26} be equal to zero represents a laminate having an infinite number of layers ($N = \infty$). It is noted from Fig. 10 that the creep deflection is more significant for a laminate with a small number of layers. In other words, the existence of the coupling relaxation moduli not only reduces the rigidity against instantaneous buckling (Tauchert, 1987), but also makes the laminates more vulnerable to the creep. The influence of the layer number on the creep deflection diminishes very rapidly as layer number

increases. The creep deflections corresponding to an eight-layer laminate are almost identical to the creep deflections of a laminate assumed to be consisted of an infinite number of layers. Therefore, it is possible to analyze the viscoelastic responses of regular, antisymmetric laminates having a large number of layers by neglecting the coupling relaxation moduli. This simplification will provide a great advantage for the analysis since the laminate is treated to be an orthotropic plate.

CONCLUDING REMARKS

The geometrically nonlinear analysis of creep responses for cross-ply and angle-ply composite laminates under in-plane compression has been conducted using the viscoelastic approach. The influence of physical aging effect on the viscoelastic behaviors of laminates is also considered. The effective time theory is employed to construct the stress–strain relation for each lamina. Consider the case that every component of creep compliances in each lamina has an identical aging shift rate, the analysis is conducted on the effective time scale. The resulting solutions are then transformed back on the real time scale. The structural responses are governed by the compatibility equation and moment equilibrium equation. The Laplace transform of the stress function can be obtained from the compatibility equation using the Laplace transform. The inverse Laplace transform of the stress function is accomplished by using the numerical integrations. The moment equilibrium condition is approximately satisfied by invoking the Galerkin method; the resulting equation is solved by the trapezoid integration rule. The creep responses of glass-reinforced bis-phenol A vinyl ester (glass/BPA) laminates are reported. The results based on the quasi-elastic analysis are also included for comparison. Based on the numerical examples, it can be concluded that:

(1) The effect of viscoelastic properties of glass/BPA on the creep responses is seen to be significant. Several examples indicate that creep deflections can reach a magnitude in the order of thickness within a few days of loading.

(2) The influence of physical aging effect is very important for a laminate under a long period of compression. The neglect of aging effect results in overestimating the creep responses.

(3) For the material considered in this study, the pre-loading aging, although does not affect the instantaneous structural responses, will slow down the creep process.

(4) For both cases when the compressive loading exceeds the instantaneous buckling load and when laminates have a large amplitude of imperfection, a large instantaneous deflection occurs once loading is applied. Consequently, the history of stress resultant variation bears a resemblance to a constant step loading. The results based on the much simpler quasi-elastic analysis agrees well with the viscoelastic solutions.

(5) For the case of laminates having small imperfections and under a loading smaller than the instantaneous buckling load, there is a large discrepancy between quasi-elastic and viscoelastic solutions. Generally, the quasi-elastic analysis predicts a faster growth in deflection. The quasi-elastic analysis also reveals a critical time at which a discernible buckling occurs. Nevertheless, it is unlikely to be true according to the more realistic viscoelastic analysis. The creep deflection history depends strongly on the magnitudes of imperfections. For a laminate with an extremely small imperfection, the laminate yields significant deflections only after a very long period of loading. Also, a gradual transition of deflection from the regime of small deflection to the large-deflection regime is observed; the transition is not drastic enough to be characterized as a buckling.

(6) The creep deflection history is seen to be very sensitive to the magnitude of loading. The deflection creeps much slower for a laminate under a smaller loading.

(7) A preliminary study on antisymmetric laminates shows that the existence of the coupling relaxation moduli can make the laminate more susceptible to the creep.

Finally, it needs to mention that the current analyses is restricted to the material systems whose aging shift rates μ_{ij} corresponding to each component of the creep compliances have an identical value. For the materials with $\mu_{22} \neq \mu_{66}$ as reported by Gates and Feldman (1995), the present stress function approach in conjunction with the Laplace transform can

not apply. This is because the relationships between the stress resultants and strains involve two effective time scales λ_{22} and λ_{66}, which makes it impossible to perform the Laplace transform. Different approaches are required for this type of materials. For example, approximating all the displacements using series of functions and applying the Galerkin method or the principle of virtual work gives a set of equations containing convolution integrals. The resulting equations are then solved for the displacement parameters using the numerical integration scheme.

Acknowledgements—The support of this research by the National Science Council of Taiwan, Republic of China through Grant NSC85-2212-E-019-004 is gratefully acknowledged.

REFERENCES

Boley, B. A. and Weiner, J. H. (1985) *Theory of Thermal Stresses*, Krieger, FL.

Brinson, L. A. and Gates, T. S. (1995) Effects of physical aging on long term creep of polymers and polymer matrix composites. *International Journal of Solids and Structures* **32,** 827–846.

Christensen, R. M. (1982) *Theory of Viscoelasticity: An Introduction*. Academic Press, New York.

Gates, T. S. and Feldman, M. (1995) Time-dependent behavior of a graphite/thermoplastic composite and the effects of stress and physical aging. *Journal of Composites Technology and Research* **17,** 33–42.

Huang, N. N. (1994) Viscoelastic buckling and postbuckling of circular cylindrical laminated shells in hygro-thermal environment. *Journal of Marine Science and Technology* **2,** 9–16.

Kim, C. G. and Hong, C. S. (1988) Viscoelastic sandwich plates with cross-ply faces. *Journal of Structural Engineering*, **114,** 150–164.

Marques, S. P. C. and Creus, G. J. (1994) Geometrically nonlinear finite element analysis of viscoelastic composite materials under mechanical and hygrothermal loads. *Computers and Structures* **53,** 449–456.

Shalev, D. and Aboudi, J. (1991) Postbuckling analysis of viscoelastic laminated plates using higher-order theory. *International Journal of Solids and Structures*, **27,** 1747–1755.

Struik, L. C. E. (1978) *Physical Aging in Amorphous Polymers and Other Materials*. Elsevier, New York.

Sullivan, J. L., Blais, E. L. and Houston, D. (1993) Physical aging in the creep behavior of thermosetting and thermoplastic composites. *Composite Science and Technology*, **41,** 389–403.

Tauchert, T. R. (1987) Thermal buckling of thick antisymmetric angle-ply laminates. *Journal of Thermal Stresses*, **10,** 113–124.

Timoshenko, S. P. and Gere, J. M. (1961) *Theory of Elastic Stability*. McGraw-Hill, New York.

Uemura, M. and Byon, O. I. (1977) Secondary buckling of a flat plate under uniaxial compression. Part 1: theoretical analysis of simply supported flat plate. *International Journal of Non-linear Mechanics*, **12,** 355–370.

Wilson, D. W. and Vinson, J. R. (1984) Viscoelastic analysis of laminated plate buckling. *AIAA Journal*, **22,** 982–988.